JOURNAL OF OPTOELECTRONICS AND ADVANCED MATERIALS, Vol. 12, No. 6, June 2010, p. 1333 - 1337

DC conduction mechanism in vanadium doped ZnTe thin films

M. S. HOSSAIN[a*], R. ISLAM[b], K. A. KHAN[b]
[a]*Department of Physics, Rajshahi University of Engineering and Technology (RUET), Rajshahi-6204, Bangladesh*
[b]*Department of Applied Physics & Electronic Engineering, University of Rajshahi, Rajshahi-6205, Bangladesh*

Vanadium doped zinc telluride (ZnTe:V) thin films (containing 2.5 to 10wt% V in ZnTe matrix) and its sandwich structures of thickness 100 to 200 nm were prepared onto glass substrate by e-beam evaporation technique in vacuum at a pressure of 8×10^{-4} Pa. The deposition rate of the films was 2.05 nms^{-1}. X-ray diffraction technique exhibits that the thin films are mixed crystalline in nature. Surface morphological studies were carried out by using SEM technique. This study indicates that the surface of ZnTe:V thin films are dense, smooth and have a compact in structure. EDAX method was used to analyze the compositions of ZnTe:V thin films. The elemental compositions of ZnTe:V films are found to follow the non-stoichiometric in nature. The dc conduction mechanism of Al/ZnTe:V/Al sandwich structure was studied in detail in the temperature range of 303 to 393 K under dc electric field of 6.67×10^{5} to 3.33×10^{8} Vm^{-1}. The dc conduction mechanism is found to obey ohmic behavior in the low field region and a modified Poole-Frenkel behavior is found to exhibit in the high field region. This study of ZnTe:V films may help in view of their technological applications in optoelectronic devices.

(Received February 18, 2010; accepted June 16, 2010)

Keywords: ZnTe:V thin films, E-beam technique, Sandwich structure, SEM, EDAX

1. Introduction

Recently there has been a growing interest in the II-VI family of semiconductors because of their potential use in photovoltaic and photoelectrochemical properties. ZnTe is of particular interest due to its low cost and high absorption co-efficient for application to photovoltaic and photoelectrochemical cells [1-4]. ZnTe is a direct band gap of 2.2 to 2.3 eV at room temperature and usually a p-type semiconductor. Literature report [5] indicates that ZnTe exhibits improved photorefractive response when it is doped with vanadium. Vanadium is believed to be a deep donor in ZnTe and its theoretical studies suggest that it plays significant role in both ZnTe and CdTe where it appears in a divalent state and occupies a cation site [6, 7]. It has attractive use in a variety of applications, including optical power limiting, holographic interferometry, optical computing and optical communications [5, 7].

Although their have been a number of investigations on the electrical [8, 9], optical [10, 11] and electro-optical [7, 10, 11] properties of the ZnTe films and ZnTe:V films [5, 6], no systematic study appears to have been done on the conduction mechanism at varying deposition conditions, in particular using vanadium as a dopant. Hence, there is a need to study the conduction mechanism of V-doped ZnTe thin films to assess its usefulness in variety of optoelectronic devices. In this paper, we discussed the preparation of ZnTe:V thin films, sandwich structure and the conduction mechanism of sandwich structure under varying dc electric field from 6.67×10^{5} to 3.33×10^{8} Vm^{-1} in the temperature range of 303 to 393 K. Obtaining results are explained in terms of various conduction models.

2. Experimental

Vanadium doped Zinc Telluride (ZnTe:V) thin film has been produced onto glass substrate by electron beam bombardment technique in vacuum at ~ 8×10^{-4} Pa from a mixture of ZnTe powder (99.999% pure) and vanadium powder (99.999% pure), respectively, obtained from Aldrich Chemical Company, USA. ZnTe:V thin films (containing 2.5 to 10wt% V) of thicknesses 100 to 200 nm were deposited, respectively. The deposition rate of films was maintained at 2.05 nms^{-1}. When the chamber pressure reduced to ~ 8×10^{-4} Pa, deposition was then started with beam current 40-50 mA by turning on the low-tension control switch of electron beam supply (EBS) unit. The lower Al (Aluminum) and upper Al electrodes were evaporated during separate pump down cycle. Three masks (one for ZnTe:V and other two for electrodes) were used for deposition of sandwich devices. All the films were deposited at room temperature. Annealing was performed at a temperature of 473 K for duration of 3 hours. The film thickness was measured by the Tolansky interference method [12] with an accuracy of ±5 nm.

I-V characteristics of sandwich Al/ZnTe:V/Al devices were measured as a function of temperature in the 303 to 393 K ranges under dc electric field. A dc power supply (Heathkit, Model: IP-2717A) was used to pass a dc current through the test sample. An electrometer (Keithly, Model: 614) was used to measure the potential differences across each sample. Digital multimeter (Model: DL-711) was also used to measure the current.

The structure of ZnTe:V thin films of different compositions as well as thicknesses for both the as-

deposited annealed films, respectively, were examined by x-ray diffraction (XRD) technique using the monochromatic CuKα radiation in the an apparatus, RINT 2200, Rigaku, Japan. Peak intensities were recorded corresponding to 2θ values. Figs. 1(a) and (b) illustrate the XRD spectra of a 150 nm thick as-deposited and annealed ZnTe:V thin films of composition 2.5wt% V onto glass substrate, respectively. In Fig. 1(a), three peaks are observed at 2θ values of 34.16°, 39.26° and 42.85°, respectively. These peaks correspond to the phases with plane V_6O_{11} (022), Zn (100) and $ZnTeO_3$ (124), respectively. These phases and planes are found from the JCPDS cards [13-15], respectively. For annealed ZnTe:V film, four peaks are observed at 2θ values of 31.67°, 34.37°, 36.26° and 41.69°, which correspond to V_4O_9 (410), V_2O_5 (310), Zn (002) and ZnTe (220) phases with plane, respectively. These phases and planes are also found from the JCPDS cards [16, 17, 14, 18], respectively.

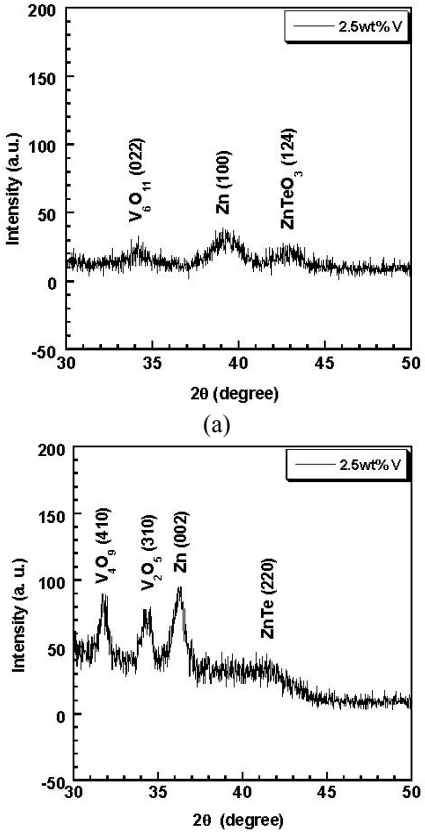

Fig. 1. XRD spectra for a 150 nm thick (a) as-deposited and (b) annealed ZnTe:V thin films of composition 2.5wt% V.

In annealed condition, the XRD peaks show up more prominently than that of as-deposited one. This could be attributed to the more crystalline nature of the annealed films. Moreover, the XRD study shows a number of oxide phases present in the author's samples. This oxide phases are formed after deposition by oxygen particles absorbed from the environment replacing one or two of the host elements in ZnTe:V. So, examination of both as-deposited as well as annealed ZnTe:V thin films exhibits that the structure of the author's sample is of a mixed crystalline in nature.

The surface morphology of the as-deposited and annealed ZnTe:V thin films were obtained by scanning electron microscopy (SEM) using Philips, Model: XL-30, operated at accelerating 10 KV potential. Figures 2(a) and (b) show the SEM micrographs of a 100 nm thick ZnTe:V as-deposited and annealed thin films of composition 2.5wt% V, respectively. From both the micrographs, it shows that the films are dense, smooth and have a compact structure. In the case of as-deposited ZnTe:V thin films, a few numbers of small-size-dots or pits were observed distributed randomly over the whole sample whereas, after annealing, the dots or pits were removed and a very smooth surface morphology was obtained. Due to limitation of available SEM system, it was not possible to capture high magnification images of our samples.

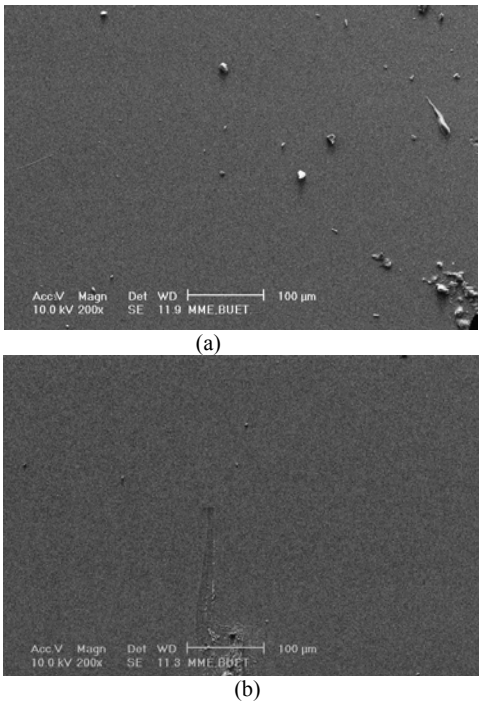

Fig. 2. SEM photographs for a 100 nm thick (a) as-deposited and (b) annealed ZnTe:V thin film of composition 2.5wt% V.

The analysis of the chemical compositions for the as-deposited as well as annealed ZnTe:V thin films of thickness 100 nm were estimated by using the method of energy dispersive analysis of x-ray (EDAX). The results are shown in Table 1. It is seen from Table 1 that for a 100 nm thick as-deposited and annealed ZnTe:V samples, the elemental composition of V and Zn do increase in annealed case compared to that of as-deposited one, whereas, the Te composition is seen to decrease in annealed case. So, the EDAX study suggests that author's ZnTe:V samples are non-stoichiometric in nature.

Table 1 Estimated elemental composition of V, Zn and Te (wt%) by EDAX method for a 100 nm thick films.

Composition (wt% V)	V (wt%)	Zn (wt%)	Te (wt%)	Remarks
2.5	2.63(±0.51)	41.98(±0.59)	55.39(±1.02)	As-deposited
2.5	3.55(±0.41)	42.45(±0.43)	54.00(±1.07)	Annealed

3. Results and discussion

There have been numerous reports [19-22] on the dc conduction behavior of the evaporated dielectric films and most results show that the current exhibits a field dependence of the form

$$I \propto exp(b\,E^{1/2}) \tag{1}$$

where E is the electric field, $b = \beta/kT$ and β is called the field lowering co-efficient [21] given by $\beta = (e^3/a\pi\varepsilon\varepsilon_o)^{1/2}$ with $a = 1$ for normal Poole-Frenkel emission (β_{PF}) and $a = 4$ for Schottky emission (β_S), k is the Boltzmann constant, ε is dielectric constant of the material, ε_o (= 8.85×10^{-12} Fm^{-1}) is the permittivity of free space and T is the absolute temperature, respectively.

The Schottky emission is the emission of electrons from the metal or semiconductor electrode into the conduction band of an insulator by thermal activation over the field-lowered metal-insulator interfacial barrier. This is also an electrode-limited conduction process. Since the author's system is a structure based on Al/ZnTe:V/Al devices, the dc conduction study of this work is divided into two parts. In the low field region (0.1-1.0 V), it corresponds to electric field range ($6.67\times10^5 \le 6.67\times10^6$ Vm^{-1}) and in the high field region (1.0-50 V), which corresponds to electric field ($6.67\times10^6 \le 3.33\times10^8$ Vm^{-1}) ranges. Figure 3 shows a typical I-V characteristics of a 150 nm thick annealed Al/ZnTe:V/Al structure of 2.5wt% V composition in the low field range. This curve shows that current and applied voltage relationship is ohmic in this voltage range. At low voltage where injection of carriers into the semicoducting material is negligible, Ohm's law is obeyed.

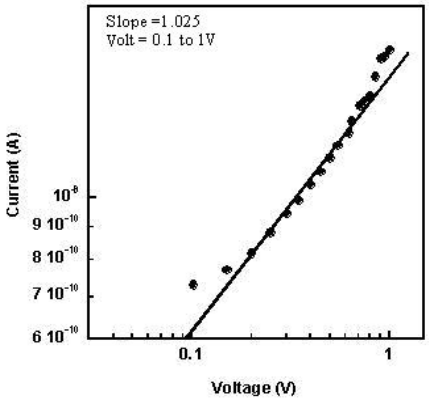

Fig. 3. Ohmic behavior for a 150 nm thick ZnTe:V thin film of composition 2.5wt% V at low field.

In high field region ($6.67\times10^6 \le 3.33\times10^8$ Vm^{-1}) author's attempt was to examine the nature of the conduction mechanism in terms of various theories based on Schottky or Poole-Frenkel emission [23]. The theory of normal Poole-Frenkel was originally put forward by Frenkel. It is a bulk-like conduction process. In this process, emission of electrons occurs from trapping centres in semiconductor and insulator by the joint effect of temperature and electric field. It is also called field assisted thermal ionization. Hence it is theoretically possible to differentiate between the Schottky and normal Poole-Frenkel emissions in thin film insulator via the different rates of change of conductivity with electric field strength, i.e. a graph of log I vs. $E^{1/2}/kT$ results a straight line with slope β_S or β_{PF}, depending on whether the conduction process is Schottky or normal Poole-Frenkel. These experimentally determined slopes can be compared with the theoretical values of β_S and β_{PF}, provided that the reasonable dielectric constant for the materials is known. Alternatively, the dielectric constant may be determined from the slopes if the controlling mechanism is known. Moreover, using metals with different work functions slopes will be symmetric for Poole-Frenkel but asymmetric for Schottky because it is an electrode-limiting process.

Using Eq. (1) a plot of log I vs. $E^{1/2}$ for a 150 nm thick Al/ZnTe:V/Al device of a composition 2.5wt% V at high field region is shown in Fig. 4. The β values of the slopes corresponding to the temperatures of 303, 333, 363 and 393 K, respectively are tabulated in the first row of Table 2.

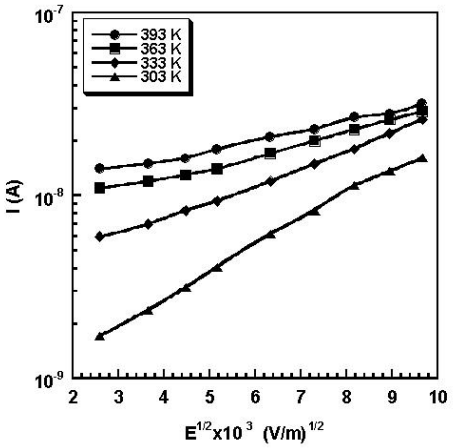

Fig. 4. Plot of log I vs. $E^{1/2}$ for a 150 nm thick Al/ZnTe:V/Al device of a composition 2.5wt% V at various temperatures at high field region.

It may be noted that Eq. (1) represents the Schottky or normal Poole-Frenkel emission process but a number of modifications have been suggested by several investigators [24, 25]. If it assumed that the insulator contains shallow neutral traps or donor centers which lie below the Fermi-level, the bulk *I-V* characteristics of the sample will be of the form an anomalous Poole-Frenkel current ($I_{(PF)AN}$)

$$I_{(PF)_{AN}} = I_o \exp\left[\frac{\beta_{PF} E^{1/2}}{2kT}\right] \tag{2}$$

where I_o is given by

$$I_o = e\mu n_c \left(\frac{N_d}{N_t}\right) E \exp\left(-\frac{E_d + E_t}{2kT}\right) \tag{3}$$

where N_d/N_t is the ratio of concentrations of donor centers to the trapping centers, E_d and E_t are the energy levels of the conduction bands. Thus the coefficient of $E^{1/2}/kT$ is

$$\frac{\beta_{PF}}{2} = \beta_S \tag{4}$$

even though the conductivity is not electrode limited, which explains the anomalous results. To explain the anomalous value of β, Hill [25] made a detailed analysis of electrical conduction in amorphous solids. The basis of analysis is ionization of local defects by an applied field. Jonscher [19] and Hartke [26] have extended Hill's model to a three-dimensional well over which all emission probabilities have to be integrated. Considering an approach of Jonscher's modification, the flow of current is to postulate that the liberated carriers travel for a constant period of time before being retrapped. This would lead to a relation

$$I \propto I_o E^{1/2} \left(\frac{kT}{e\beta_{PF}}\right) exp(e\beta_{PF} E^{1/2}/kT) \tag{5}$$

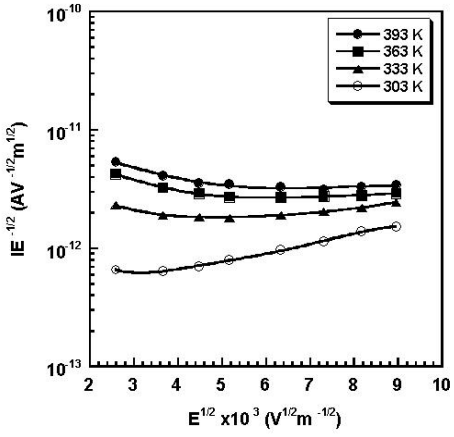

Fig. 5. Plot of log $IE^{-1/2}$ vs. $E^{1/2}$ for a 150 nm thick Al/ZnTe:V/Al device of a composition 2.5wt% V at various temperatures at high field region.

According to Eq. (5), the curves of log($IE^{-1/2}$) vs. $E^{1/2}$ were plotted for different temperatures and they are shown in Fig. 5. The β values of the slopes corresponding to the temperatures of 303, 333, 363 and 393 K, respectively are illustrated in the second row of Table 2.

Considering another approach of Jonscher's modification, the flow of current can be written as the following relation

$$I \propto I_o \left(\frac{kT}{e\beta_{PF} E^{1/2}}\right) \exp(e\beta_{PF} E^{1/2}/kT) \tag{6}$$

Using Eq. (6), a plot of log ($IE^{1/2}$) vs. $E^{1/2}$ for a 150 nm thick Al/ZnTe:V/Al structure of composition 2.5wt% V in the high field region is shown in Fig. 6. The calculated theoretical and experimental β values as well as their corresponding evaluated values of dielectric constants are tabulated in third row of Table 2.

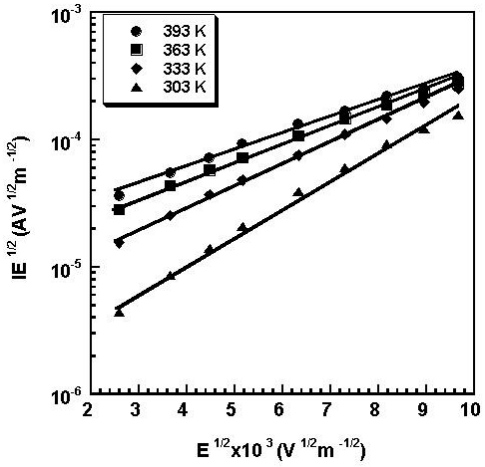

Fig. 6. Plot of log $IE^{1/2}$ vs. $E^{1/2}$ for a 150 nm thick Al/ZnTe:V/Al device of a composition 2.5wt% V at various temperatures at high field region.

In order to identify the exact mechanism existing in the present system, theoretical field-lowering co-efficients β_S and β_{PF} are calculated by taking the high frequency dielectric constant ε of ZnTe:V film as 10.017, obtained from the author's dielectric studies and this value is agreed well with the reported [5] value.

From the Table 2, it is seen that for normal Poole-Frenkel case, author's experimental average value of β under the temperature 303 to 393 K lies between the theoretical values of β_{PF} and β_S. This value does not fit close to any of the β values. Now for the case of Jonscher's model (log $IE^{-1/2}$ vs. $E^{1/2}$), the author's experimental average β value lies even below of their corresponding theoretical value of β_{PF} and β_S. From Table 2, it is also noticed that for Jonshcer's model (log $IE^{1/2}$ vs. $E^{1/2}$) case, corresponding average experimental value of β, i.e. 2.37×10^{-5} ($eVm^{1/2}V^{-1/2}$) in the temperature 303 to 393 K, is very close to the corresponding theoretical value

of $\beta_{PF,}$ i.e. 2.39×10^{-5} ($eVm^{1/2}V^{-1/2}$). The results, therefore, suggest that the conduction mechanism of author's sample follows the modified Poole-Frenkel mechanism (modified as Jonscher's model).

Table 2 Experimental and theoretical values of field-lowering coefficients.

Temperature (K)	Experimental $\beta\times10^{-5}$ ($eVm^{1/2}V^{-1/2}$)	Theoretical $\beta_{PF}\times10^{-5}$ ($eVm^{1/2}V^{-1/2}$)	Theoretical $\beta_{S}\times10^{-5}$ ($eVm^{1/2}V^{-1/2}$)	Experimental (ε)	Remarks
303	1.82	2.39	1.195	17.27	Schottky Model or Normal Pool-Frenkel Model (log I vs. $E^{1/2}$)
333	1.51			25.09	
363	1.21			39.08	
393	1.01			56.09	
303	1.28	2.39	1.195	34.92	Jonscher's Model (log $IE^{-1/2}$ vs. $E^{1/2}$)
333	0.93			66.15	
363	0.57			176.11	
393	0.53			203.69	
303	2.49	2.39	1.195	9.28	Jonscher's Model (log $IE^{1/2}$ vs. $E^{1/2}$)
333	2.39			10.02	
363	2.33			10.54	
393	2.27			11.10	

4. Conclusion

Vanadium doped ZnTe thin film sandwich structures (containing 2.5 to 10wt% V in ZnTe matrix) of thickness in the range 100 to 200 nm were prepared onto glass substrate by e-beam evaporation in vacuum at a pressure of 8×10^{-4} Pa. The deposition rate of the films was at about 2.05 nms^{-1}. X-ray diffraction technique was used to study the structure of the film and it was found that the films are mixed crystalline in nature. Surface morphological studies suggest that the author's sample are smooth, dense and compact in nature. The elemental composition was estimated by EDAX method which suggests that the author's samples are non-stoichiometric in nature. The Al/ZnTe:V/Al film structure was studied in the temperature range of 303 to 393 K under dc electric field. The conduction mechanism is found to follow ohmic behavior in the low field and modified Poole-Frenkel behavior in the high field region.

Acknowledgement

One of the author's M. S. Hossain is indebted to Rajshahi University of Engineering & Technology, Bangladesh for providing the study leave during this work.

References

[1] A. J. Nozik, R. Memming, J. Phys. Chem. **100**, 13061 (1996).
[2] J. O. M. Bockris, K. Uosaki, J. Electrochem. Soc. **124**, 1348 (1977).
[3] K. K. Mishra, K. Rajeshwar, J. Electroanal. Chem. **273**, 169 (1978).
[4] D. Ham, K. K. Mishra, K. Rajeshwar, J. Electrochem. Soc. **138**, 100 (1991).
[5] M. Ziari., W. H. Steier, P. M. Ranon, Appl. Phys. Lett. **60**, 1052 (1992).
[6] J. Kreissl, K. Irmscher, Phys. Rev. **B 53**, 1917 (1996).
[7] A. Zunger, Solid State Physics, FL Academic Press, Orlando, p.276 (1989).
[8] H. Dong-Hun, C. Shin-Jung, P. Su-Moon, J. Electrochem. Soc. **150**, C342 (2003).
[9] A. K. S. Aqili, Z. Ali, A. Maqsood, Appl. Surf. Sci. **167**, 1 (2000).
[10] H. Bellakhder, A. Outzourhit, E. L. Ameziane, Thin Solid Films **382**, 30 (2001).
[11] R. L. Gunshor, L. A. Kolodziejski, N. Otsuka, S. Datta, Surf. Sci. **174**, 522 (1986).
[12] S. Tolansky, Multiple Beam Interferometry of Surfaces and Films, Oxford University Press (1948).
[13] J. Andersson , K. Arkiv, JCPDS Card No 18-1451, **21,** 413 (1964).
[14] T. Swansun, DC Fel, JCPDS Card No 4-0831, Reports, **60** (1951).
[15] K. Frank, University of Leningrad, USSR, Saturiwiss, JCPDS Card No 20-1270, **54,** 199 (1967).
[16] W. Karl-Axel, W. Kjell, Acta Chem Scan, JCPDS Card No 24-1391, **24,** 3409 (1970).
[17] Nat. Bur., Standards CIRC, JCPDS Card No 9-387, **8,** 66 (1958).
[18] Nat. Bur., Stds. U.S. Mono., JCPDS Card No 15-746, **25,** 58 (1964).
[19] A. K. Jonscher, Thin Solid Films, **1**, 213 (1967).
[20] A. K. Jonscher, J Electrochem Soc. **116,** C217 (1969).
[21] M. Deery, J. G. Perkins, K. G. Stephens, Thin Solid Films, **8,** R16 (1971).
[22] H. H. Poole, Phil. Mag. **33**, 112 (1916); **34**, 195 (1917).
[23] J. Frenkel, J Phys Rev. **54**, 647 (1938).
[24] J. G. Simmons, Phys Rev. **155,** 657 (1967).
[25] R. M. Hill, Thin Solid Films, **8,** R21 (1971).
[26] J. L. Hartke, J Appl Phys. **39,** 4871 (1968).

*Corresponding author: sazzad_phy@yahoo.com